Eur. Phys. J. D **42**, 133–137 (2007)
DOI: 10.1140/epjd/e2007-00014-0

THE EUROPEAN PHYSICAL JOURNAL D

Phase sensitive parametric amplification of optical vortex beams

F. Devaux[a] and R. Passier

Institut FEMTO-ST, Département d'Optique P.M. Duffieux, Unité Mixte de Recherche 6174 du CNRS, Université de Franche-Comté, 25030 Besançon Cedex, France

Received 21 February 2006 / Received in final form 28 November 2006
Published online 24 January 2007 –

Abstract. Optical vortex beams with different topological charges are amplified in a travelling wave phase sensitive parametric interaction. Amplified beams observed either in the near field or in the far field domains exhibit patterns that depend on the relative phase between the pump and the vortex beams. Experimental results are compatible with the conservation of orbital angular momentum of the input beam whatever phase matching conditions.

PACS. 42.65.Yj Optical parametric oscillators and amplifiers – 41.85.Ct Beam shaping, beam splitting

1 Introduction

While optical tweezers technologies become mature and relevant for some applications like light-driven micromachines [1] and optical manipulation of particles [2], generation and propagation of optical vortex (OV) beams in non linear media and properties of optical vortex beams involved in non linear interactions experience a growing interest during the last years. While OV is usually obtained in a linear regime with passive optical elements, $\chi^{(2)}$ non linear media can also be used to generate beams with orbital angular momentum (OAM) either in a traveling wave parametric optical amplifier (OPA) [3] or in an optical parametric oscillator (OPO) [4]. Soliton-propagation of OV in various non linear media [5–9], conservation or transfer of the OAM in up or down conversion [10–12] and simultaneous frequency up-conversion and beam shaping of optical tweezers in second harmonic (SH) interaction [13] seriously enlarge perspectives for future promising applications of OV.

This paper deals with the experimental parametric amplification of OV in a degenerate type 1 OPA. Since it has been proved that OAM is transferred to the idler wave in a type 2 OPA when either the pump or the signal beams are OV [12], sensitivity to the relative phase between the pump and the signal beams in a degenerate type 1 OPA [14,15] also involves reshaping of OV carried by the signal beam like in a seeded SH interaction [13]. Indeed, in a degenerate type 1 OPA, the amplification gain in the transverse plane depends on the pump beam profile as well as the relative phase between interacting beams. It leads to amplification or de-amplification that reshapes the signal beam in its transverse plane. Then, new various patterns are obtained depending on phase matching condition, topological charge of the vortex and wave front of the pump beam.

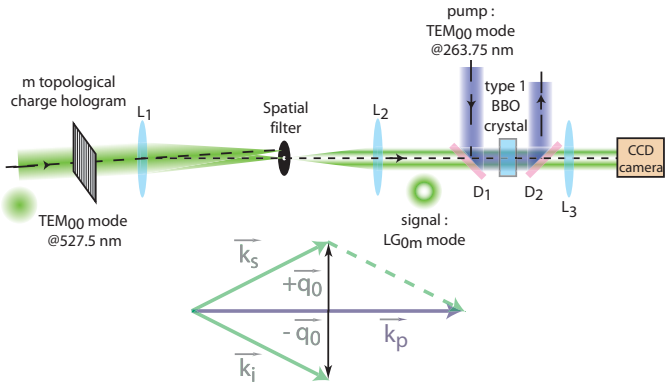

Fig. 1. (Color online) Experimental set-up. L_1, L_2 and L_3: convergent lenses. D_1, D_2: dichroic mirrors (T_{max} at 527.5 nm and R_{max} at 263.75 nm). TEM_{00} Gaussian beam illuminates an amplitude computed hologram. The diffraction order carrying an orbital angular momentum is selected with a spatial filter. The collimated vortex beam is amplified in a type 1 BBO crystal and imaged onto a CCD camera. Wave vectors describe a non collinear phase matched interaction between pump, signal and idler waves.

2 Experimental results

Figure 1 sketches the experimental set-up. The optical vortex is prepared by illuminating a computed amplitude hologram with a pulsed Gaussian beam of 1 ps time duration at $\lambda_s = 527.5$ nm delivered by a frequency doubled Q-switch mode-locked Nd:glass laser (Twinkle, Light Conversion Inc.). The diffracted light is focused and spatially

[a] e-mail: fabrice.devaux@univ-fcomte.fr

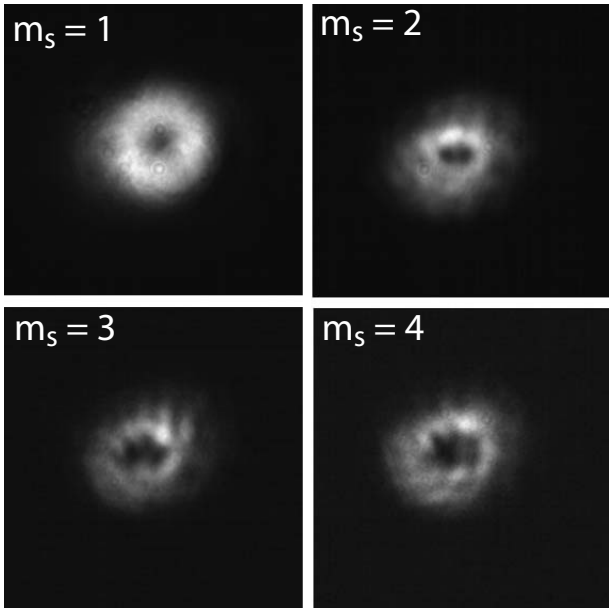

Fig. 2. Images of non amplified vortex beams with topological charges $m_s = 1, 2, 3, 4$.

filtered in order to select the diffraction order that gives a Laguerre-Gauss beam carrying a topological charge m_s. The collimated vortex beam (i.e. the signal) is amplified in a 4 mm long type 1 BBO crystal by a pump beam at $\lambda_p = 263.75\,\text{nm}$ corresponding to the 4th harmonic of the laser (at the degeneracy $2\lambda_p = \lambda_s$). The size of the pump beam is enlarged with a telescope to ensure an uniform amplification gain in the whole transverse section of the crystal. Then, near field of the vortex beam is observed by imaging the input face of the crystal onto a single-shot CCD camera. Far field is observed by placing the CCD camera onto the focal plane of the lens L_3.

Figure 2 represents pictures of non amplified vortices with topological charges $m_s = 1, 2, 3, 4$ obtained with different holograms. For $m_s = 1$, the diameter of the dark core of the vortex is about $100\,\mu$m.

In a degenerate type 1 OPA, the intensity of the amplified beam detected on the CCD camera results from the coherent superposition of the signal and the idler waves. Lets assume that the amplitude of the pump plane wave is constant in the transverse plane. In the undepleted pump approximation, when no idler wave is present at the crystal input, amplitudes of the output signal and idler waves are given by [14]:

$$\begin{cases} A_s^{out} = \left(\cosh(bL) + i\frac{\Delta k}{2b}\sinh(bL)\right) A_s^{in} \\ A_i^{out} = -i\frac{g}{2b}\sinh(bL) A_s^{in*} \end{cases} \quad (1)$$

where $A_s^{in}(\overrightarrow{r}) = A_0(\overrightarrow{r})e^{i\Delta\phi(\overrightarrow{r})}$ is the amplitude of the input vortex beam and $\Delta\phi(\overrightarrow{r}) = \phi_s(\overrightarrow{r}) - \phi_p(\overrightarrow{r})$ corresponds to the relative phase in the transverse plane between the pump and the signal waves at the crystal input. With g related to the pump amplitude and $\Delta k = |\Delta\overrightarrow{k}| = |\overrightarrow{k}_p - \overrightarrow{k}_s - \overrightarrow{k}_i = \overrightarrow{0}|$ corresponding to the phase mismatch ($\overrightarrow{k}_p$, $\overrightarrow{k}_s$, $\overrightarrow{k}_i$ are respectively the wave vectors of the pump, signal and idler waves), b is defined like $b = \frac{1}{2}\sqrt{g^2 - \Delta k^2}$ when $g > \Delta k$. L is the crystal length. For perfect phase matching ($\Delta k = 0$), equations (1) become:

$$\begin{cases} A_s^{out} = \cosh(\frac{gL}{2})A_s^{in} = \sqrt{G}A_s^{in} \\ A_i^{out} = -i\sinh(\frac{gL}{2})A_s^{in*} = -i\sqrt{G-1}A_s^{in*} \end{cases} \quad (2)$$

where G is the amplification gain. In the high gain regime ($G \gg 1$), coherent superposition of the signal and idler waves leads to an amplitude of the output beam in the transverse plane given by:

$$\begin{aligned} A^{out}(\overrightarrow{r}) &= A_s^{out}e^{i\overrightarrow{q_0}\cdot\overrightarrow{r}} + A_i^{out}e^{-i\overrightarrow{q_0}\cdot\overrightarrow{r}} \\ &\simeq 2\sqrt{G}A_0(\overrightarrow{r})e^{-i\frac{\pi}{4}}\cos\left[\Delta\phi + \overrightarrow{q_0}\cdot\overrightarrow{r} + \frac{\pi}{4}\right]. \end{aligned} \quad (3)$$

Intensity is:

$$I_{OV}^{out}(\overrightarrow{r}) \simeq 2GI_{OV}^{in}(\overrightarrow{r}) \times (1 - \sin[2\Delta\phi + 2\overrightarrow{q_0}\cdot\overrightarrow{r}]), \quad (4)$$

where I_{OV}^{in} is intensity of OV at the crystal input. $\overrightarrow{q_0}\cdot\overrightarrow{r}$ denotes the influence of a collinear or a non collinear scheme on the process (see Fig. 1). In a collinear scheme where $\overrightarrow{q_0} = \overrightarrow{0}$, the amplification process depends only on the relative phase $\Delta\phi$. When $\Delta\phi = -\frac{\pi}{4}$ modulo π, output intensity is $I_{OV}^{out} \simeq 4GI_{OV}^{in}$, and corresponds to amplification of the signal with a maximum gain. When $\Delta\phi = +\frac{\pi}{4}$ modulo π, intensity is $I_{OV}^{out} \simeq 0$. Then intensity of the output beam is modulated according to the variation of the relative phase $\Delta\Phi$ in the transverse plane. When $\overrightarrow{q_0} = \overrightarrow{0}$, equation (3) shows that phase in the transverse plane of the amplified beam is constant and is respectively equal to $-\frac{\pi}{4}$ in areas where $\cos(\Delta\Phi + \frac{\pi}{4}) > 0$ and to $\frac{3\pi}{4}$ in areas where $\cos(\Delta\Phi + \frac{\pi}{4}) < 0$. It corresponds to a π phase shift between amplified areas.

In the high gain regime, equation (3) presupposes that phase singularity no more exists in the amplified beam and that could lead to the assumption that "degenerate collinear OPA destroys the vortex" [11] and suggests an apparent paradox of non-conservation of angular momentum in spontaneous parametric down conversion [10]. But if we consider the exact calculation of the total angular momentum of the output beam which results from the superposition of two coaxial singular beams of opposite charges [19]:

$$L_z^{out} = L_{zs}^{out} + L_{zi}^{out} \propto \iint \{m_s|A_s^{out}|^2 + m_i|A_i^{out}|^2\} d^2\overrightarrow{r} \quad (5)$$

where L_{zs}^{out} and L_{zi}^{out} are angular momentum of the output signal and idler beams and m_s and m_i are topological charges associated to these beams. Since $m_i = -m_s$ [12] and by considering equations (1), it leads to:

$$L_z^{out} \propto \iint m_s|A_s^{in}|^2 d^2\overrightarrow{r} \equiv L_{zs}^{in} \quad (6)$$

whatever the amplification gain, amplitude of the phase mismatch and amplitude of $\overrightarrow{q_0}$. It means that total angular momentum carried by the output beam in the near

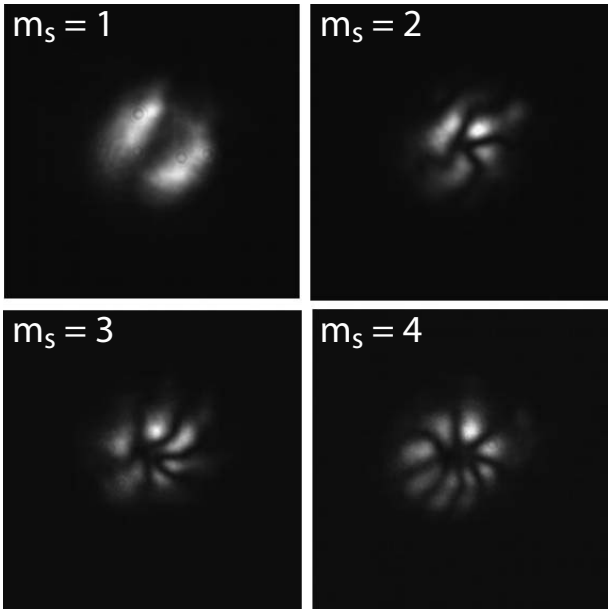

Fig. 3. Flower-like patterns of the amplified vortex beams obtained with a collinear phase-matched interaction and with a pump plane wave. The number N of petals is connected to the topological charge m of the vortex by $N = 2m$.

field for collinear or non collinear, phase matched or phase mismatched interactions is equal to the total angular momentum of the input signal beam and proves that angular momentum of the signal is always conserved in optical parametric interaction whatever phase matching conditions.

Figure 3 shows the amplified OV beams when the pump beam is a plane wave. Flower-like patterns are obtained. Indeed, the relative phase is given by:

$$\Delta\phi(\overrightarrow{r}) = m_s\theta(\overrightarrow{r}) + \theta_0, \tag{7}$$

where $\theta(\overrightarrow{r})$ is the azimuth angle and θ_0 is the mean value of the relative phase in the transverse plane. Hence, amplified OV exhibit "petals" centered on azimuth angles where $\Delta\phi(\overrightarrow{r}) = -\frac{\pi}{4}$ modulo π. The number N of petals is connected to the charge m_s of the input vortex by $N = 2|m_s|$. From one laser shot to another, rotation of flower-like patterns is observed. This rotation is due to the shot-to-shot fluctuation of the mean value of the relative phase θ_0 between the pump and the signal beams.

Figure 4 shows interference patterns obtained with an amplified OV beam with a topological charge $m_s = 1$ in a collinear interaction. In a high gain regime, when perfect phase matching occurs, Figure 4a shows continuous fringes between the two amplified petals with no phase dislocation and the π phase shift between the amplified areas is revealed by the spatial shift of fringes between the amplified areas. Interference pattern suggests that no more phase singularity exists in the amplified output beam. Actually, in high gain regime, interference contribution of the remaining input phase singularity in the amplified output field is negligible (see Eq. (4)). In Figure 4b amplification gain is reduced by introducing a small phase mismatch.

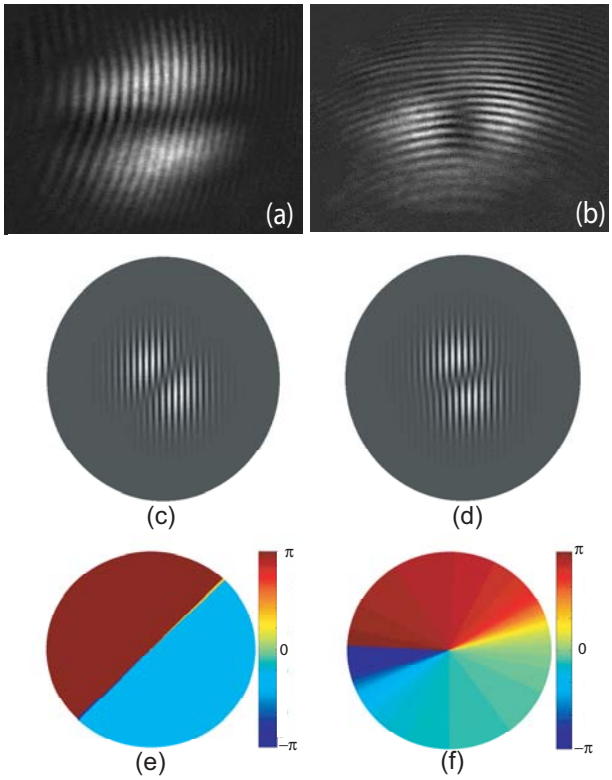

Fig. 4. (Color online) Experimental interference patterns of amplified OV with charge $m_s = 1$ for perfectly phase matched (a) and mismatched (b) collinear interaction. Numerical simulations of interference patterns and phase maps of amplified OV for perfectly phase matched (c, e) and mismatched (d, f) collinear interactions.

Then, contribution of the remaining input phase singularity in the interference pattern becomes significant and can be observed with a good contrast. Experimental results can be compared to numerical simulations presented by Figures 4c and 4d. When origin of phase is taken along the horizontal axis, amplified areas are in the azimuthal directions $-\frac{\pi}{4}$ and $\frac{3\pi}{4}$ for perfect phase matching. When phase mismatch occurs, constant additional phase related to the phase mismatch amplitude changes phase origin that induces rotation of amplified areas (Fig. 4d). Figures 4e and 4f show the corresponding calculated phase maps of the amplified OV. Figure 4e clearly shows the π phase shift between amplified areas revealed by the interferogram. In this case remaining input phase singularity can not be observed. When phase mismatch occurs, phase map (Fig. 4f) shows that input phase singularity is retrieved.

For a pump wave with a spherical wavefront, the expression of the relative phase becomes for a collinear interaction:

$$\Delta\phi(\overrightarrow{r}) = m_s\theta(\overrightarrow{r}) + \theta_0 - \frac{2\pi}{\lambda_p}\frac{r^2}{R_p} \tag{8}$$

where λ_p is the wavelength and R_p the wavefront curvature radius of the pump wave at the input of the crystal. For example, points in the transverse plane for which

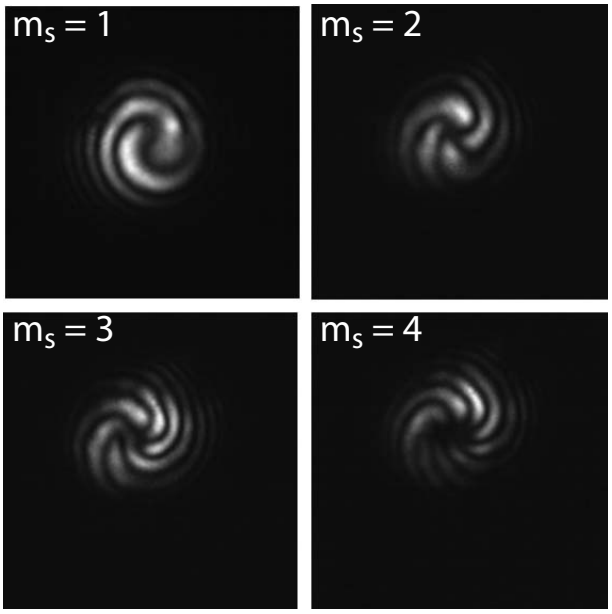

Fig. 5. Spiral patterns of the amplified vortex beams obtained with a collinear phase-matched interaction and a spherical pump wave.

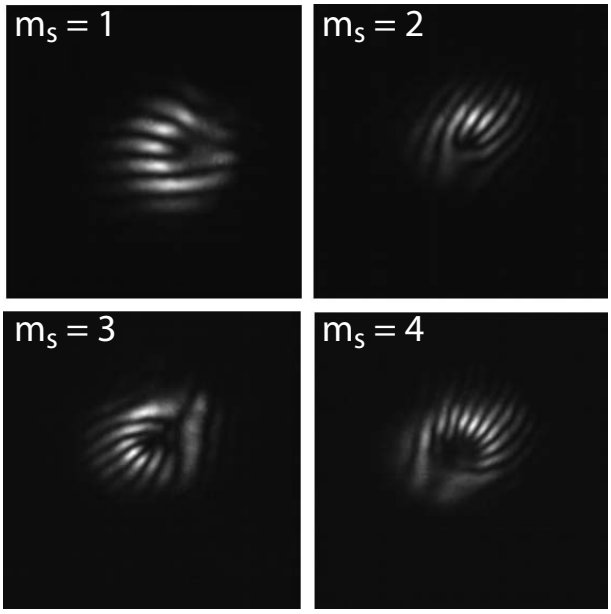

Fig. 6. Patterns of amplified vortex beams obtained in a non collinear phase-matched interaction with a pump plane wave.

$\Delta\phi = 0$ correspond to an isophasic curve that obeys to the equation $r^2 = \frac{\lambda R_p}{2\pi}(m_s\theta + \theta_0)$. It corresponds to the equation of a spiral. Figure 5 presents experimental images of OV amplified by a spherical pump wave. Petals in the previous experimental scheme where the pump was a plane wave become spirals where bright fringes correspond to the isophasic lines $\Delta\phi = -\frac{\pi}{4}$ modulo π. Patterns in Figure 5 are analogous to patterns observed when an optical vortex beam interfere with a spherical wave [16] but here, the number of arms in the spirals is twice the vortices charge.

Another kind of patterns can be obtained for a non collinear interaction between the signal and a pump plane wave ($\overrightarrow{q_0} \neq 0$). Then equation (4) leads to patterns where the intensity of amplified OV beams is modulated by interference fringes showing a topological defect characteristic of phase singularities.

Figure 6 presents images of amplified OV beams obtained with a non collinear interaction and a pump plane wave. Orientation and periodicity of interference fringes depend on the direction and the amplitude of $\overrightarrow{q_0}$ (see Eq. (4)). Fringes patterns are connected to topological charges of the different input beams and are analogous to interference patterns observed when two vortices of opposite charges interfere [17].

When amplified vortex beams are observed in the far field domain (Fourier plane) analog patterns are observed for perfectly phase matched collinear interaction. Petals or spirals are observed when the pump beam is respectively a plane (Fig. 7a) and a spherical (Fig. 7b) wave.

When perfectly phase matched non collinear interaction is considered in the high gain regime ($\overrightarrow{q_0} \neq 0, G \gg 1$), amplitude of the output beam can be expressed in the far field like:

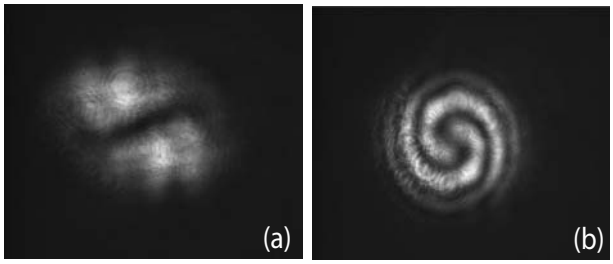

Fig. 7. Far field patterns of amplified vortex beams with $m_s = 1$ for collinear phase matched interaction with a pump plane wave (a) or spherical wave (b).

$$\tilde{A}^{out}(\overrightarrow{q}) = \sqrt{\tilde{G}(\overrightarrow{q})}\tilde{A}_s^{in}(\overrightarrow{q} - \overrightarrow{q_0}) - i\sqrt{\tilde{G}(\overrightarrow{q}) - 1}\tilde{A}_s^{in*}(\overrightarrow{q} + \overrightarrow{q_0}), \quad (9)$$

where $\tilde{G}(\overrightarrow{q})$ is the amplification transfer function in the spatial frequencies domain [18] and $\tilde{A}_s^{in}(\overrightarrow{q})$ is the far field amplitude of the input vortex beam. It gives two separated vortices of opposite charge respectively centered on spatial frequencies $+\overrightarrow{q_0}$ and $-\overrightarrow{q_0}$.

Figure 8a shows the interferometry pattern of an amplified vortex beam ($m_s = 1$) observed in the far field for a non collinear phase matched interaction. Fringes clearly exhibit the opposite charges of the signal and the idler beams. While in the near field we define OAM around the propagation axis; in the far field, we calculate OAM carried by each beam around the spatial frequencies $+\overrightarrow{q_0}$ and $-\overrightarrow{q_0}$ over areas that include only one beam. If we suppose that the amplification gain is a constant in the limit of the spatial frequencies bandwidth of the amplification transfer function [18] ($\tilde{G}(\overrightarrow{q}) \simeq G$), then amplified signal and

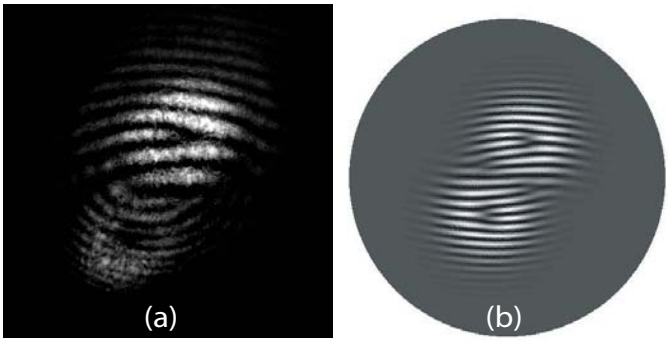

Fig. 8. Experimental result (a) and numerical simulation (b) of far field pattern of amplified vortex beams with $m_s = 1$ for a non collinear phase matched interaction. Interferometric technique reveals the opposite OAM carried by the signal and the idler and additional phase singularities of opposite sign can be observed between the colliding beams.

idler beams carry respectively a total angular momentum:

$$\begin{cases} L_{zs}^{out} = GL_{zs}^{in} \\ L_{zi}^{out} = -(G-1)L_{zs}^{in} \end{cases}. \tag{10}$$

In the near field corresponding pattern (Fig. 6, $m_s = 1$) signal and idler are indistinguishable and total OAM carried by the amplified beam is equal to the total OAM of the input beam and do not depend on $\overrightarrow{q_0}$ (see Eq. (6)) but in the far field domain, OAM carried by the output signal beam is amplified. When the transverse component $\overrightarrow{q_0}$ is tuned (i.e. changing the propagation direction of the signal beam with respect to the pump one), amplified signal and idler vortices move symmetrically to each other around the zero spatial frequency associated to the direction of the pump beam. When $\overrightarrow{q_0}$ tends to zero, signal and idler vortices collide and analog phenomena related in reference [20] are observed: interferogram reveals additional phase singularities of opposite sign between the colliding beams. Figure 8b shows the corresponding numerical simulation where additional phase singularities are clearly exhibited.

3 Conclusion

In conclusion, we experimentally performed the parametric phase sensitive amplification in a degenerate type 1 crystal of optical vortex beams with different topological charges in the high gain regime. Various patterns corresponding to the interference between the amplified signal and the idler waves have been observed with respect to experimental conditions either in the near field or in the far field domains. Flower-like and spiral patterns are obtained in both domains for collinear interactions when the pump beam is respectively a plane or a spherical wave. The number of petals or spirals in patterns is connected to the charges of vortices and correspond to isophasic lines in the transverse plane where relative phase between the pump and the signal waves is equal to $-\frac{\pi}{4}$ modulo π. Results of phase analysis in near field of the amplified output beam by interferometric technique are compatible with the conservation of the total OAM in degenerate type 1 parametric interaction whatever phase matching conditions.

References

1. H. Rubinsztein-Dunlop, M.E.J. Friese, Opt. Photon. News **13**, 22 (2002)
2. M.P. MacDonald, L. Paterson, K. Volke-Sepulveda, J. Arlt, W. Sibbett, K. Dholakia, Science **296**, 1101 (2002)
3. P. Di Trapani, A. Beržanskis, S. Minardi, S. Sapone, W. Chinaglia, Phys. Rev. Lett. **81**, 5133 (1998)
4. A.V. Smith, D.J. Armstrong, Opt. Expr. **11**, 868 (2003)
5. G.A. Swartzlander Jr, C.T. Law, Phys. Rev. Lett. **69**, 2503 (1992)
6. G. Duree, M. Morin, G. Salamo, M. Seguev, B. Crosignani, P. Di Porto, E. Sharp, A. Yariv, Phys. Rev. Lett. **74**, 1978 (1995)
7. B. Luther-Davies, R. Powles, V. Tikhonenko, Opt. Lett. **19**, 1816 (1994)
8. Z. Chen, M. Segev, D.W. Wilson, R.E. Muller, P.D. Maker, Phys. Rev. Lett. **78**, 2948 (1997)
9. P. Di Trapani, W. Chinaglia, S. Minardi, A. Piskarskas, G. Valiulis, Phys. Rev. Lett. **84**, 3843 (2000)
10. K. Dholakia, N.B. Simpson, M.J. Padgett, Phys. Rev. A **54**, R3742 (1996)
11. A. Beržanskis, A. Matijošius, A. Piskarskas, V. Smilgevičius, A. Stabinis, Opt. Comm. **140**, 273 (1997)
12. D.P. Cætano, M.P. Almeida, P.H. Souto Ribeiro, J.A.O. Hugenin, B Coutinho dos Santos, A.Z. Khoury, Phys. Rev. A **66**, 041801-1 (2002)
13. G. Molina-Terriza, L. Torner, S. Minardi, P. Di Trapani, J. Mod. Opt. **50**, 1563 (2003)
14. F. Devaux, E. Lantz, J. Opt. Soc. Am. B **12**, 224 (1995)
15. F. Devaux, E. Lantz, Phys. Rev. Lett. **85**, 2308 (2000)
16. I.V. Basistiy, M.S. Soskin, M.V. Vasnetsov, Opt. Comm. **119**, 604 (1995)
17. V. Pyragaite, A. Stabinis, Opt. Comm. **220**, 247 (2003)
18. F. Devaux, E. Lantz, Opt. Comm. **114**, 295 (1995)
19. M.S. Soskin, V.N. Gorshov, M.V. Vasnetsov J. T. Malos, N.R. Heckenberg, Phys. Rev. A **56**, 4064 (1997)
20. G. Molina-Terriza, J. Recolons, L. Torner, Opt. Lett. **25**, 1135 (2000)